View Article Online / Journal Homepage / Table of Contents for this issue

Synthesis and properties of chiral imidazolium ionic liquids with a (1*R*,2*S*,5*R*)-(−)-menthoxymethyl substituent†‡

Juliusz Pernak,*[a] Joanna Feder-Kubis,[a] Anna Cieniecka-Rosłonkiewicz,[b] Cedric Fischmeister,[c] Scott T. Griffin[d] and Robin D. Rogers*[d]

Received (in Cambridge, UK) 7th December 2006, Accepted 24th January 2007
First published as an Advance Article on the web 21st February 2007
DOI: 10.1039/b616215k

A series of 1-[(1*R*,2*S*,5*R*)-(−)-menthoxymethyl]-3-alkylimidazolium salts have been synthesized, producing both hydrophilic and hydrophobic chiral imidazolium ionic liquids. Their physicochemical properties, single-crystal X-ray structures, antimicrobial activities, and antielectrostatic effects were determined and these compounds have proven to represent not only potential new solvents in asymmetric synthesis, but also effective, disinfectants with antielectrostatic activity. Given the number and diversities of the possible conformations and interionic interactions, coupled with the chiral nature of the cations, it should come as no surprise that these salts exhibit ionic liquid behavior and are so difficult to crystallize.

Introduction

Ionic liquids (ILs) are now well known as salts with melting points below 100 °C, and typically have broad liquid ranges, low vapor pressures, and may be both non-coordinating, but highly polar. They are receiving considerable global attention because they offer a unique environment for chemistry, biocatalysis, separation science, material synthesis, and electrochemistry.[1] Among several classes of ILs, the newest class are chiral ionic liquids (CILs).[2–18] They have attracted significant attention due to their potential application in chiral discrimination, asymmetric synthesis, and optical resolution of racemates.[19,20] Very few methods for the synthesis of CILs have been described,[9,13–18] and their real potential in asymmetric synthesis remains to be proven.

Chirality in these salts can arise from either the anion or the cation. For example, a CIL in which the chirality was related to the anion, was used as the solvent in an asymmetric Diels–Alder reaction.[3] In the same reaction, a CIL with a chiral cation was used as a Lewis acid.[2] Good yields and significant enantiomeric excesses were obtained when ammonium CILs were used as reaction media in the enantioselective version of the Baylis–Hillman reaction[21] and aza-Baylis–Hillman reaction.[22] The best enantioselectivity was obtained (44%) when the Baylis–Hillman reaction was performed for seven days. Also, several CILs have been successfully used as chiral solvents in the photoisomerization of dibenzobicyclo[2.2.2]octatriene diacid to induce enantiomeric excesses.[23] The observed enantioselectivities, though modest in an absolute sense, are among the highest achieved for unimolecular photochemical reactions by use of a chiral environment.[23]

Successful procedures for the preparation of ILs containing a chiral anion have been reported; including lactates[3,11] and amino acids.[24] In the literature, however, many more examples are noted of CILs in which chirality is related to the cation. These are mainly imidazolium-,[9,12,13,23] ammonium-,[4,13,14,21,23,25] pyridinium-[26] and oxazolium-based[4] ILs.

In this study, we present the synthesis and properties of imidazolium CILs directly obtained from the natural chiral pool of (1*R*,2*S*,5*R*)-(−)-menthol. Menthol, characterized by its sharp, penetrating smell, belongs to the family of saturated, monocyclic, terpene alcohols. It has eight isomers, the structures and names of which are listed in Scheme 1. Peppermint or cornmint oil represents a rich source of menthol, obtained from various varieties of mints (*Menthae* L.), in which it can comprise as much as 50% of the oil's weight. It exhibits a soothing, anesthetic effect on mucous membranes and is widely used in cosmetic and pharmaceutical industries. (1*R*,2*S*,5*R*)-(−)-Menthol is a popular commercial and relatively inexpensive isomer.

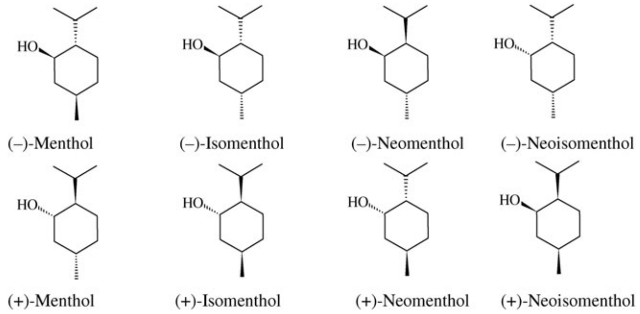

Scheme 1 Isomers of menthol.

---

[a] *Poznań University of Technology, Poznań, Poland*
[b] *Institute of Industrial Organic Chemistry, Warsaw, Poland*
[c] *CNRS-Université de Rennes 1, Rennes, France*
[d] *Department of Chemistry and Center for Green Manufacturing, The University of Alabama, Tuscaloosa, AL 35487, USA*

† The HTML version of this article has been enhanced with colour images.

‡ Electronic supplementary information (ESI) available: ^{1}H and ^{13}C NMR data and elemental analysis for **1d–l**, **2b–l**, **8b–l** and Table of close contact interactions for **1a–1c** (Table S1). See DOI: 10.1039/b616215k

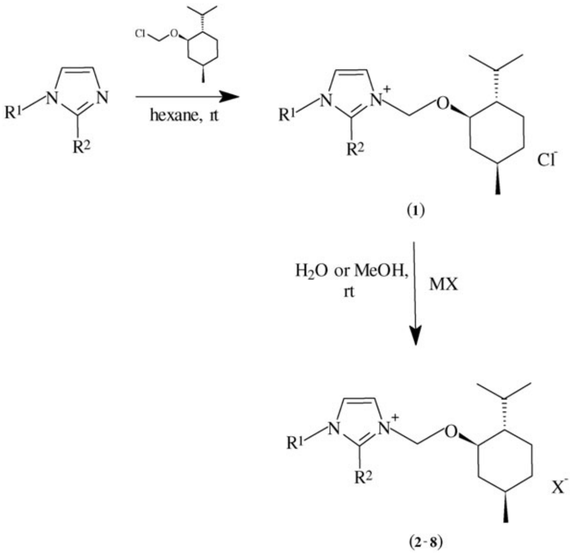

Scheme 2

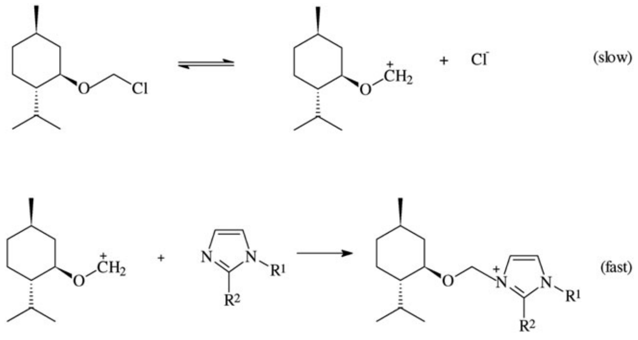

Scheme 3

Results and discussion

Syntheses

A series of chiral imidazolium salts of $[Cl]^-$, $[BF_4]^-$, $[ClO_4]^-$, $[I]^-$, $[PF_6]^-$, $[Ace]^-$ (acesulfamate), $[CF_3COO]^-$, and $[Tf_2N]^-$ were prepared (Scheme 2) and their properties were determined. First, the 1-alkylimidazoles shown in Table 1 were prepared by the reactions of imidazole with the appropriate alkyl bromides in the presence of base (sodium in 1-propanol). Quaternization was achieved using freshly distilled 1-alkylimidazole and distilled chloromethyl (1*R*,2*S*,5*R*)-(−)-menthyl ether. This ether is an excellent reagent, but it is readily hydrolyzed to HCl, CH_2O, and menthol. In view of this, these reactions should be conducted under strictly anhydrous conditions. Here, a suitable solvent proved to be anhydrous hexane; from which the product precipitated. (In the cases of 1,2-dimethylimidazole and 1-benzylimidazole, dry DMF and dry acetone were used, respectively.)

The quaternization proceeded *via* a specific type of Menschutkin reaction involving an S_N1 mechanism. The initial rate-determining step was identified as involving formation of the cation, as show in Scheme 3. The cation thus formed then reacted very rapidly with 1-alkylimidazole.

The synthesized chiral imidazolium chlorides (**1**, Table 2) were obtained in very good yields and their specific rotations were measured. The purities of these salts were determined by a direct two-phase titration technique (EN ISO 2871-2: 1994) and ranged from 97.5 to 99.9% (Table 2). The remainder was essentially water, since the chlorides are strongly hygroscopic. The chloride salts with methyl and ethyl substituents (**1a**, **1b** and **1m**, respectively) manifested the highest melting temperatures. Adding longer alkyl substituents resulted in a rapid decrease in melting temperatures until oils were obtained.

Metathesis reactions of the chloride salts were carried out using KBF_4, $NaClO_4$, KI, $NaPF_6$, K(Ace) and $NaCF_3CO_2$. Chiral imidazolium salts of $[BF_4]^-$, $[ClO_4]^-$, $[I]^-$, $[PF_6]^-$, $[Ace]^-$ and $[CF_3COO]^-$ were obtained as crystalline materials with sharply defined melting temperatures. Table 3 lists the melting temperatures, specific rotation, and surfactant contents as estimated by a direct two-phase titration technique, using methanol as solvent. On the basis of the melting temperatures, all of the salts listed in Table 3, except for **4** and **5**, can be considered as CILs.

The new salts are water insoluble with the exception of the $[Ace]^-$ and $[CF_3COO]^-$ salts. Melting temperatures were anion dependent as illustrated by the 1-[(1*R*,2*S*,5*R*)-(−)-menthoxymethyl]-3-methylimidazolium salts: $[Cl]^-$ (**1a**) mp = 137–138 °C, $[I]^-$ (**4**) mp = 127–129 °C, $[PF_6]^-$ (**5**) mp = 125–126 °C, $[BF_4]^-$ (**2a**) mp = 99–102 °C, $[ClO_4]^-$ (**3**) mp = 98–99 °C, $[Ace]^-$ (**6**) mp = 62–63 °C, and $[CF_3COO]^-$ (**7**) mp = 20–21 °C. The length of the alkyl substituent showed an even greater effect on melting points as shown for $[Cl]^-$ and $[BF_4]^-$ salts. The chloride salt with R^1 = methyl (**1a**) melted at 137–138 °C, while the chloride salt, R^1 = undecyl (**1k**) was an oil at room temperature. Similarly, the $[BF_4]^-$ salt with R^1 = methyl (**2a**) and R^1 = undecyl (**2k**) had melting points of 99–102 and 28–30 °C, respectively.

All of the $[Tf_2N]^-$ salts (**8**) are chiral imidazolium room temperature ionic liquids (RTILs); the 12 representatives of which are listed in Table 4. These hydrophobic salts were dried in vacuum at 80 °C for 24 h and stored over P_4O_{10}. The water contents, determined by Karl-Fischer measurements, were found to be less than 500 ppm. After 41 days, these anhydrous

Table 1 Prepared 1-alkylimidazoles

R^1	Yield (%)	Bp/°C	R^1	Yield (%)	Bp/°C
CH_3	91	76–77 @ 18 mmHg	C_7H_{15}	81	153–154 @ 31 mmHg
C_2H_5	85	97–98 @ 27 mmHg	C_8H_{17}	83	151–152 @ 16 mmHg
C_3H_7	83	89–90 @ 18 mmHg	C_9H_{19}	78	174–175 @ 27 mmHg
C_4H_9	90	114–116 @ 12 mmHg	$C_{10}H_{21}$	85	172–173 @ 25 mmHg
C_5H_{11}	74	119–120 @ 20 mmHg	$C_{11}H_{23}$	79	167–168 @ 16 mmHg
C_6H_{13}	79	135–136 @ 24 mmHg	$C_{12}H_{25}$	83	199–200 @ 24 mmHg

Table 2 1-[(1*R*,2*S*,5*R*)-(−)-Menthoxymethyl]-2,3-dialkylimidazolium chlorides (**1**)

Chloride	R^1	R^2	Yield (%)	Mp/°C	Surfactant content (%)	Specific rotation[f] $>\alpha]_D^{20}$
1a	CH_3	H	96.5	137–138[a]	97.9	−116.6 (*c* = 0.9)
1b	C_2H_5	H	89.5	144–145[a]	97.8	−111.4 (*c* = 1.0)
1c	C_3H_7	H	74.0	73–74[b]	98.2	−97.6 (*c* = 1.2)
1d	C_4H_9	H	96.0	83–84[c]	97.4	−95.5 (*c* = 1.0)
1e	C_5H_{11}	H	99.0	55–58[d]	98.5	−92.7 (*c* = 1.0)
1f	C_6H_{13}	H	97.5	44–46[d]	99.3	−87.4 (*c* = 0.3)
1g	C_7H_{15}	H	99.5	Oil	97.5	−84.5 (*c* = 0.6)
1h	C_8H_{17}	H	99.5	Oil	97.5	−79.5 (*c* = 1.1)
1i	C_9H_{19}	H	97.0	Oil	99.6	−75.2 (*c* = 0.7)
1j	$C_{10}H_{21}$	H	97.0	Oil	99.5	−74.4 (*c* = 1.4)
1k	$C_{11}H_{23}$	H	99.0	Oil	99.9	−73.5 (*c* = 0.6)
1l	$C_{12}H_{25}$	H	99.0	Oil	99.9	−73.0 (*c* = 1.0)
1m	CH_3	CH_3	99.0	200–203[e]	98.1	−118.3 (*c* = 1.0)
1n	CH_2Ph	H	99.5	67–69[c]	97.9	−93.7 (*c* = 1.3)

[a] From ethyl acetate–acetone–ethanol, needles. [b] From ethyl acetate, large needles. [c] From ethyl acetate–acetone, plates. [d] From ethyl acetate, plates. [e] From ethyl acetate–chloroform–ethanol, plates. [f] *c* in ethanol.

CILs were found to have absorbed water from the atmosphere to a maximum level of 1.8% (Fig. 1).

The $[Tf_2N]^-$ CILs (**8**) are water insoluble, and more dense than water. The densities range from 1.14 to 1.33 g mL^{-1} and decrease with increasing molar mass. Fig. 2 shows that there is a linear relationship between the molar volume (calculated from the equation $V_m = M/d$ where d = density) and the number of carbon atoms in the imidazolium alkyl group substituent. These salts are insoluble in hexane and diethyl ether, but are soluble in acetone, chloroform, DMF, THF, ethyl acetate, toluene, DMSO, and low-molecular-weight alcohols.

The $[Tf_2N]^-$ salts are all viscous liquids. Increases in molar mass were accompanied by increases in viscosity, while increasing the temperature results in a decrease in viscosity, as shown in Fig. 3 for **8g**. Additionally,[27] as observed for other ILs, the viscosity of these $[Tf_2N]^-$ salts decrease upon addition of water or other chemical impurities.

The specific rotation and thermal properties for the CILs **8** were established by DSC and TGA analyses, and are listed in Table 4. For all these salts, the glass transition temperatures (T_g), approached −50 °C, and all were thermally stable up to *ca.* 230 °C. (The presence of oxygen decreased the decomposition temperature, as observed earlier for 1,3-dialkoxymethylimidazolium salt-based ILs.[28]) In the first stage, the menthoxy group is released, resulting in two estimated decomposition temperatures (T_d) (Table 4). The $[Tf_2N]^-$ salts could not be estimated by a direct two-phase titration technique, because the $[Tf_2N]^-$ anion in this ion pair is not interchangeable.

All synthesized salts were characterized by ^1H NMR, ^{13}C NMR, and elemental analysis. The spectra were consistent with the literature data.[14,29] Protons of the H_2C13 group, which links the two rings, appear in the spectrum in the form of two doublets. Manifestation of the diastereoisotopic protons was typical for all the studied salts, *e.g.*, for **1a** 5.69, 5.89 (d, J = 10.4 Hz, 2H, AB system).

The ^1H NMR spectra of the chlorides and the other salts indicate different chemical shifts for the imidazolium ring protons and methylene protons adjacent to the oxygen atoms (Table 5). A strong anion effect was evident. Substitution of the $[Cl]^-$ anion with $[ClO_4]^-$, $[Ace]^-$, $[I]^-$, $[BF_4]^-$, $[PF_6]^-$, $[Tf_2N]^-$ and $[CF_3COO]^-$ resulted in changes in the imidazolium ring electron density. A shift of 2 ppm between the $[Cl]^-$ salt and the $[PF_6]^-$ salt in the case of the HC12 group,

Table 3 1-[(1*R*,2*S*,5*R*)-(−)-Menthoxymethyl]-3-alkylimidazolium salts (**2–7**)

Salt	R^1	Anion	Yield [%]	Mp/°C	Surfactant content (%)	Specific rotation[b] $[\alpha]_D^{20}$
2a	CH_3	$[BF_4]^-$	99.5	99–102	97.5	−97.5 (*c* = 0.9)
2b	C_2H_5	$[BF_4]^-$	99.5	66–68	97.7	−99.3 (*c* = 0.8)
2c	C_3H_7	$[BF_4]^-$	99.5	52–54	98.2	−86.9 (*c* = 0.5)
2d	C_4H_9	$[BF_4]^-$	99.5	27–28	97.3	−78.5 (*c* = 0.6)
2e	C_5H_{11}	$[BF_4]^-$	98.5	60–61	99.9	−84.7 (*c* = 0.7)
2f	C_6H_{13}	$[BF_4]^-$	98.5	59–60.5	97.5	−72.9 (*c* = 0.9)
2g	C_7H_{15}	$[BF_4]^-$	99.0	76–78	99.9	−83.0 (*c* = 0.5)
2h	C_8H_{17}	$[BF_4]^-$	98.5	77–79	99.9	−83.6 (*c* = 0.7)
2i	C_9H_{19}	$[BF_4]^-$	99.0	70–71	96.5	−61.2 (*c* = 1.2)
2j	$C_{10}H_{21}$	$[BF_4]^-$	98.5	42–43	97.5	−72.3 (*c* = 1.1)
2k	$C_{11}H_{23}$	$[BF_4]^-$	99.5	28–30	99.9	−65.3 (*c* = 1.1)
2l	$C_{12}H_{25}$	$[BF_4]^-$	98.5	40–42	98.3	−77.8 (*c* = 0.6)
3	CH_3	$[ClO_4]^-$	99.5	98–99	97.6	−94.8 (*c* = 0.9)
4	CH_3	$[I]^-$	99.5	127–129	97.5	−86.2 (*c* = 1.0)
5	CH_3	$[PF]^-$	99.5	125–126	97.7	−81.9 (*c* = 0.9)
6	CH_3	$[Ace]^-$ [a]	98.0	62–63	98.0	−79.4 (*c* = 0.5)
7	CH_3	$[CF_3COO]^-$	97.0	20–21	97.9	−83.0 (*c* = 1.1)

[a] Acesulfamate. [b] *c* in ethanol.

Table 4 1-[(1*R*,2*S*,5*R*)-(−)-Menthoxymethyl]-3-alkylimidazolium bis(trifluoromethanesulfonyl)imides (**8**)

Salt	R	Yield (%)	Specific rotation[a] $[\alpha]_D^{20}$	Density[b]/g mL^{-1}	Viscosity[b]/mm^2 s^{-1}	T_{onset}/°C	T_d[c]/°C	T_g[d]/°C
8a	CH_3	87.9	−63.3 (*c* = 1.5)	1.33	302	230	250/470	−44
8b	C_2H_5	91.2	−65.6 (*c* = 1.0)	1.30	338	225	250/470	−46
8c	C_3H_7	87.8	−60.3 (*c* = 1.1)	1.29	379	230	250/475	−48
8d	C_4H_9	91.6	−58.7 (*c* = 2.2)	1.27	421	230	250/470	−51
8e	C_5H_{11}	94.3	−57.4 (*c* = 1.6)	1.26	444	230	250/475	−50
8f	C_6H_{13}	89.1	−59.6 (*c* = 1.1)	1.24	447	225	250/470	−50
8g	C_7H_{15}	89.9	−56.0 (*c* = 0.9)	1.22	469	230	250/475	−51
8h	C_8H_{17}	87.9	−56.7 (*c* = 1.0)	1.21	505	225	250/470	−50
8i	C_9H_{19}	93.4	−55.0 (*c* = 1.1)	1.19	542	230	250/470	−51
8j	$C_{10}H_{21}$	91.4	−51.4 (*c* = 1.2)	1.17	567	230	250/475	−51
8k	$C_{11}H_{23}$	92.1	−43.4 (*c* = 1.1)	1.15	572	230	250/470	−51
8l	$C_{12}H_{25}$	98.9	−47.1 (*c* = 1.1)	1.14	580	230	250/475	−51

[a] *c* in ethanol. [b] At 30 °C. [c] Thermal degradation temperature. [d] Glass transition temperature.

exemplifies the dramatic effect of the change in electron density resulting from changing the anion. Similar observations concerning the ring protons were made by Fannin *et al.* for 1-alkyl-3-methylimidazolium salts.[30]

Comparing the differences between values of the chemical shifts for the HC12 group, the anions can be ordered according to their increasing shielding capacities as follows:

$$[Cl]^- < [I]^- < [CF_3COO]^- < [Ace]^- < [ClO_4]^- < [BF_4]^- < [Tf_2N]^- < [PF_6]^-$$

The most pronounced shielding abilities were noted for the $[PF_6]^-$ and $[Tf_2N]^-$ anions. Additionally, the ^{13}C NMR spectra indicated notable differences in the chemical shifts depending on the anion used. These shifts were most evident for carbon C12; the differences between corresponding $[Cl]^-$ and $[Tf_2N]^-$ salts ranged from 1.5 to 3 ppm. The alkyl group substitution in position 1 of the imidazole ring also affected the shifts, *e.g.*, 1.5 ppm for CH_3 (salt **1a** and **8a**), but 3 ppm for C_2H_5 (salt **1b** and **8b**) or C_3H_7 (salt **1c** and **8c**).

Crystal structures

The crystal structures of three members of this series of compounds were determined: 1-[(1*R*,2*S*,5*R*)-(−)-menthoxymethyl]-3-methylimidazolium chloride hydrate (**1a** · H_2O), 1-[(1*R*,2*S*,5*R*)-(−)-menthoxymethyl]-3-ethylimidazolium chloride hemihydrate (**1b** · $0.5H_2O$), and 1-[(1*R*,2*S*,5*R*)-(−)-menthoxymethyl]-3-propylimidazolium chloride hemihydrate (**1c** · $0.5H_2O$). All three compounds have multiple ions in the asymmetric unit (Fig. 4), due to the variable conformations of the alkyl substituents and the menthol moiety, and the multiple, variable, and weak interionic interactions. These multiple configurations and interactions, and the chiral nature of the compounds, makes obtaining suitable single crystals for analysis difficult (see Experimental section), however, this bodes well for using these moieties to induce 'ionic liquid' behavior. Here we briefly examine these factors by looking at the cation conformations, the interionic interactions and the packing in each case.

Cation conformations. Fig. 5 illustrates with cation overlays, the distinct conformations of the menthol and alkyl groups isolated. For **1a** · H_2O, the main differences between unique cations lie in the torsion angle between the menthol and the imidazolium moieties where N2–C13–O1–C6 = −81.2(2)° for one cation (O1) and 134.3(2)° for the second cation (labeled with primes) cation (O1′).

In **1b** · $0.5H_2O$, the cations differ in two ways; the menthol orientations (C12–N2–C13–O1 = 107.4(4)° and −70.1(4)° for the unprimed and prime labeled cations (O1 and O1′, respectively) and the ethyl group orientations. In the cation containing the unprimed labeled cation (O1), the methyl end-group is 0.679(13) Å on the opposite side of the plane of the

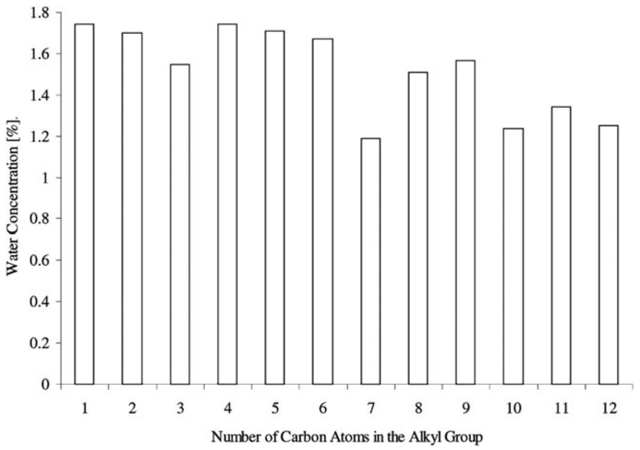

Fig. 1 Maximum water content in hydrophobic CILs **8**.

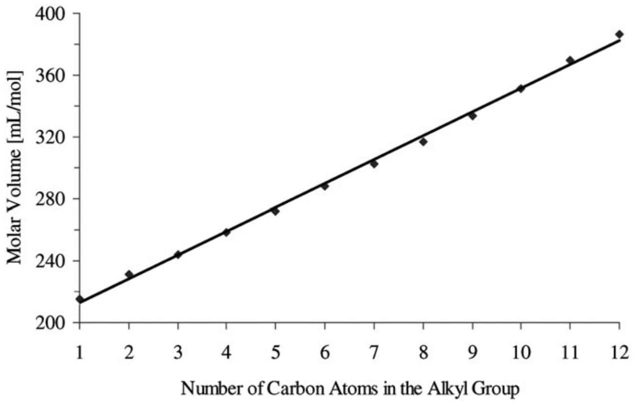

Fig. 2 Molar volume as a function of the number of carbon atoms in the alkyl group in CILs **8**.

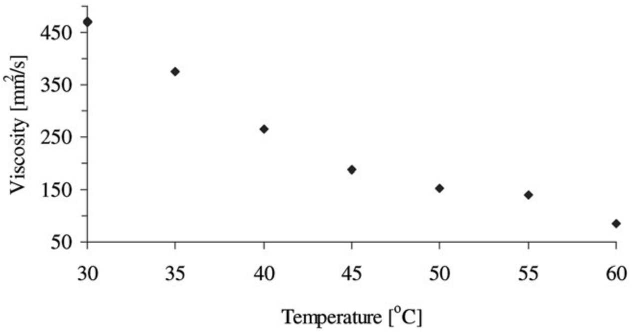

Fig. 3 Viscosity of dry CIL **8g** as a function of increasing temperature.

imidazolium ring from the menthol moiety, the only cation in this series with this feature.

1c · 0.5H$_2$O crystallizes with four cations, two solvent water molecules, and four chloride anions in the asymmetric unit. The cations can be divided into two pairs of similar orientations, one pair consisting of the cations containing oxygen atoms O1 and O1′ and the other containing O2 and O2′. The cations (O1, O1′) have the *n*-propyl group extending out away from the imidazolium ring with the N2–C10–C16–C17 torsion angle nearly linear (177(1)° av.), while in the other pair, (O2, O2′) the *n*-propyl group wraps over the imidazolium ring, on the same side as the menthol moiety with the average torsion angle being −48(1)°. It is noteworthy here (and important for the π-stacking described below), that the menthol moiety and alkyl substituent are on the same side of the imidazolium ring.

Interionic interactions. The weak interionic interactions observed include both hydrogen bonding and π-stacking. Two types of ring overlap interactions are observed (Fig. 6): face-to-face stacking (**1c** · 0.5H$_2$O) and edge overlap (**1a** · H$_2$O), while no π-overlap interactions were observed for **1b** · 0.5H$_2$O (the only structure in the series with a cation that has the menthol moiety and the alkyl substituent on opposite sides of the imidazolium ring). In **1a** · H$_2$O (edge overlap), the ring edge separations are 3.577(3) Å for C9···N1′ and 3.425(3) Å for C11···C12. (Note that this interaction does not cross the polymeric water–chloride hydrogen bonded chain in the *a* direction, but from adjacent cations along *b*.) Congestion of the menthol moieties appears to prevent the cations from further overlap.

For compound **1c** · 0.5H$_2$O, almost complete face-to-face overlap of the imidazolium rings is observed. (Note that in this structure the water–chloride hydrogen bond region is not polymeric and the imidazolium rings are able to interact across this region.) The average ring atom···ring atom contact distance is 3.49(5) Å and a very strict segregation of all ring substituents to one side of the imidazolium ring is noted for each unique cation.

In addition to the π-interactions, there are many close contacts under van der Waals separations, including hydrogen bonds between the cations, anions, and the water molecules (Fig. 7). The strongest hydrogen bond interactions are between the chloride anions and the solvate water molecules (see below), however, additional contacts are noted with the imidazolium ring hydrogen atoms, the bridging methylene hydrogen atoms, and even hydrogen atoms on the alkyl substituents.

A few inter-cation interactions are also observed in each structure. The closest such contacts include: in **1a** · H$_2$O between the menthol oxygen and hydrogen C11 on the imidazolium ring; in **1b** · 0.5H$_2$O between the menthol oxygen and the C3 hydrogen atom in the menthol ring; and in **1c** · 0.5H$_2$O between the menthol oxygen and the acidic C32 (C32′) hydrogen atom on the imidazolium ring.

The anions can be quite crowded when the cations pack with the imidazolium end pointing towards the chloride anion,

Table 5 The chemical shifts[a] in ^{1}H NMR

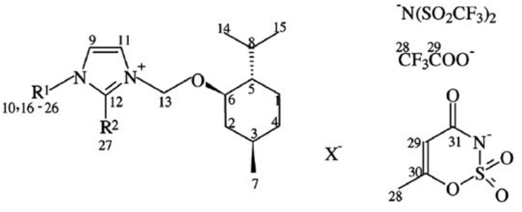

		Characteristic protons			
Salt	Anion	HC12	HC9	HC11	H$_2$C13
1a	[Cl]$^-$	10.72 (t)	7.87 (t)	7.54 (t)	5.69, 5.89 (d, *J* = 10.4)
2a	[BF$_4$]$^-$	8.90 (t)	7.46 (t)	7.44 (t)	5.52, 5.60 (d, *J* = 10.7, *J* =10.4)
3	[ClO$_4$]$^-$	9.03 (t)	7.46 (m)	7.46 (m)	5.53, 5.63 (d. *J* = 10.7. *J* = 10.4)
4	[I]$^-$	10.39 (t)	7.71 (t)	7.56 (t)	5.69, 5.89 (d, *J* = 10.4)
5	[PF$_6$]$^-$	8.65 (t)	7.41 (t)	7.36 (t)	5.49, 5.55 (d, *J* = 10.7, *J* = 10.4)
6	[Ace]$^{-\,b}$	9.87 (t)	7.57 (t)	7.52 (t)	5.60, 5.74 (d, *J* = 10.4)
7	[CF$_3$COO]$^-$	10.26 (t)	7.71 (t)	7.58 (t)	5.59, 5.75 (d, *J* = 10.4, *J* = 10.7)
8a	[N(SO$_2$CF$_3$)$_2$]$^-$	8.87 (t)	7.48 (t)	7.46 (t)	5.52, 5.59 (d, *J* = 10.4)

[a] Shift in ppm and *J* in Hz. [b] Acesulfamate.

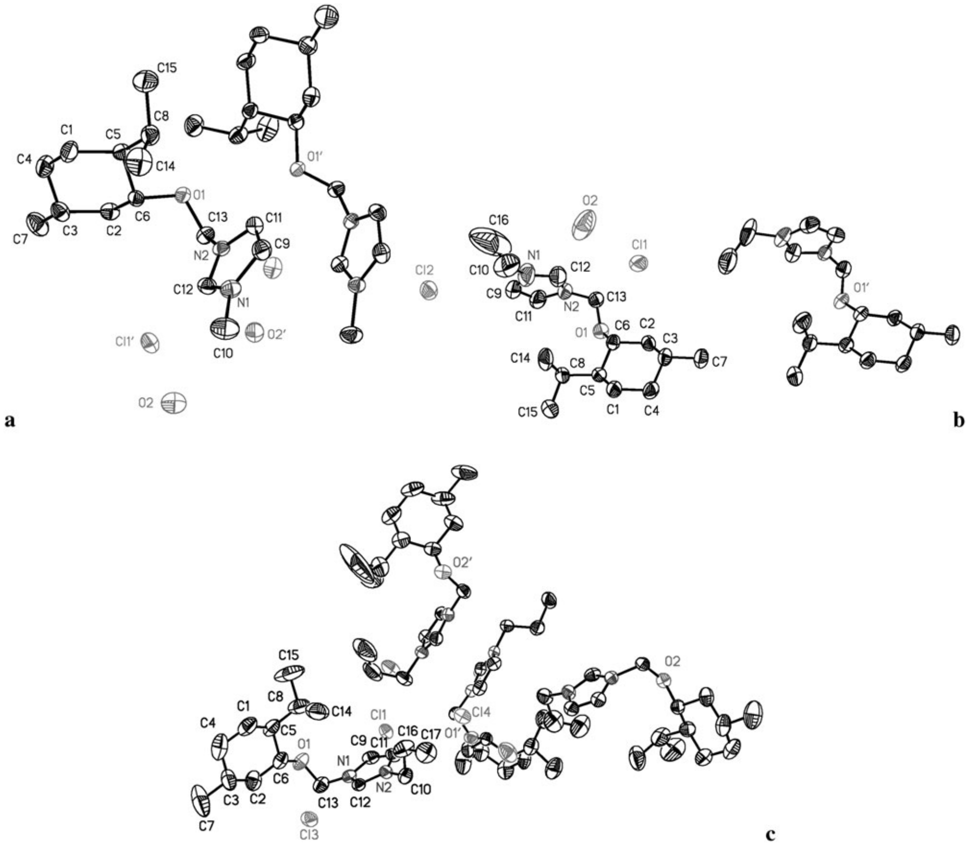

Fig. 4 ORTEP diagrams of (a) 1-[(1*R*,2*S*,5*R*)-(−)-menthoxymethyl]-3-methylimidazolium chloride hydrate (**1a** · H_2O) (top left), (b) 1-[(1*R*,2*S*,5*R*)-(−)-menthoxymethyl]-3-ethylimidazolium chloride hemihydrate (**1b** · $0.5H_2O$) (top right), and (c) 1-[(1*R*,2*S*,5*R*)-(−)-menthoxymethyl]-3-propylimidazolium chloride hemihydrate (**1c** · $0.5H_2O$) (bottom). The thermal ellipsoids are depicted at 50% probability and hydrogen atoms have been omitted for clarity. The high thermal motion indicative of conformational disorder is discussed in the Experimental section.

allowing room for three or four cations to interact with each anion. These environments can also be less crowded when the cations pack opposite and parallel to each other across the chloride anion, allowing for only two cations to interact with the anion.

Packing interactions. Packing diagrams for **1a–c** are shown in Fig. 8 and illustrate how the cations are segregated with the menthol moieties in hydrophobic regions and the imidazolium rings into more hydrophilic regions. Hydrogen bonds between the chloride anions and the water solvate molecules can be seen in the hydrophilic regions between the imidazolium rings, especially in the fully hydrated **1a** · H_2O where the water–chloride hydrogen bonds form a polymeric chain running parallel to the *b* axis between the imidazolium rings. In the hemihydrate structures, the hydrogen bonds are limited to discrete units of water molecules between two chloride anions and do not form polymeric chains. Given the number and diversities of the possible conformations and interionic interactions, coupled with the chiral nature of the cations, it should come as no surprise that these salts exhibit ionic liquid behavior and are so difficult to crystallize.

Antibacterial activities

The chiral imidazolium chlorides were tested for antimicrobial activity against rods, cocci, and fungi. Values of minimum inhibitory concentration (MIC) and minimum bactericidal or fungicidal concentration (MBC) were established and are compared in Table 6 to the corresponding values for the widely applied benzalkonium chloride (BAC), in which the alkyl group represents a mixture ranging from C_8H_{17} to $C_{18}H_{37}$.

The mean MIC and MBC values for all the studied microbes are plotted in Fig. 9. The results suggest a strong effect of the alkyl substituent chain length on biological activity. For example, the chloride salts containing alkyl substituents with more than five carbon atoms should be regarded as active, but those with nonyl, decyl, undecyl or dodecyl substituents should be regarded as superactive.

The MIC and MBC values are comparable, indicating not only a strong biostatic effect, but also high biocidal activity. Furthermore, the activities were higher than that shown by BAC and these exceptional imidazolium chlorides, thus possess, a broad spectrum of activity against microbes.

The $[I]^-$, $[CF_3COO]^-$, $[Ace]^-$, $[ClO_4]^-$, $[BF_4]^-$, $[Tf_2N]^-$ and $[PF_6]^-$ salts can also be expected to be effective against bacteria and fungi, as confirmed by the results obtained with 1-alkoxymethyl-3-methylimidazolium $[Cl]^-$, $[BF_4]^-$ and $[PF_6]^-$.[31] However, the chiral pool of (1*R*,2*S*,5*R*)-(−)-menthol does affect the antimicrobial activity, and this is also noted for lactates, where imidazolium L-lactates are more active than imidazolium DL-lactates.[11]

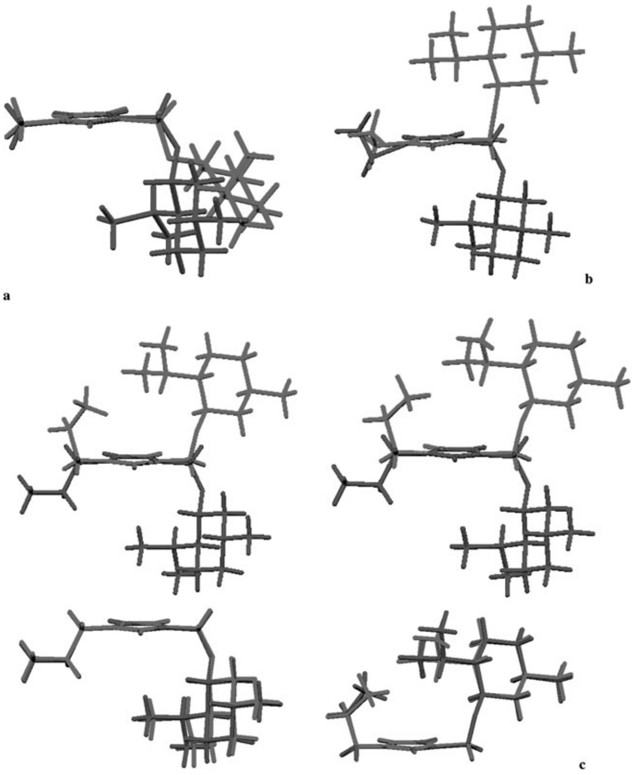

Fig. 5 Overlay of (a) the two cations in **1a** · H_2O (top left); (b) the two cations in **1b** · $0.5H_2O$ (top right); and (c) the cations in **1c** · $0.5H_2O$: O1, O2 (middle left), O1′, O2′ (middle right), O1, O1′ (bottom left), and O2, O2′ (bottom right).

Antielectrostatic effects

The antielectrostatic effects observed are a result of two quantities: the surface resistance and the half-life decay time. The surface resistance, R_s (in Ω), has been calculated from eqn (1):

$$R_s = Ul/is \quad (1)$$

where U is the applied voltage (U = 100 V), l is the length of electrodes (l = 100 mm), i is the measured current intensity (i = A), and s is the distance between the electrodes (s = 10 mm). The half-life decay time, $\tau_{1/2}$ (in s), was determined from eqn (2):

$$\tau_{1/2} = \sqrt{\frac{\tau_+^2 + \tau_-^2}{2}} \quad (2)$$

where τ_+ and τ_- are the mean half-decay times of positive and negative charges, respectively. The reported antielectrostatic effects were determined following the criteria listed in Table 7 and presented in Table 8.

The 1-[(1*R*,2*S*,5*R*)-(−)-menthoxymethyl]-3-alkylimidazolium chlorides **1a–l** demonstrated an excellent antielectrostatic effect. Their ability to drain the surface charge reflected their strong hygroscopic properties. Introduction of an additional methyl group to the imidazole ring, as well as, the presence of an aromatic ring in the molecule, markedly inhibits the draining of surface charge (Table 8, chlorides **1m** and **1n**). However, the $[BF_4]^-$ salts **2**, do not exhibit antielectrostatic properties. A similar absence of effect was observed for the one studied representative of the $[ClO_4]^-$, **3**, and $[PF_6]^-$, **5**, salts.

On the other hand, the $[Tf_2N]^-$ salts, **8**, even if strongly hydrophobic, demonstrated a strong tendency to drain the surface charge. Thus, it is not the hydrophobic character, but the state of aggregation which plays a significant role. Until now, hygroscopic liquids or greasy substances have been thought to be excellent antielectrostatic agents. Given our results however, attention should certainly be given to hydrophobic ionic liquids which are potentially effective antielectrostatic agents.

Conclusions

By applying Menschutkin reaction conditions, a number of chiral imidazolium-based ILs were synthesized, in which the chirality originates from the cation, which was derivatized form the natural chiral pool of (1*R*,2*S*,5*R*)-(−)-menthol. All the obtained salts are stable in air, water, and commonly used organic solvents. These ILs also included RTILs containing the $[Tf_2N]^-$ anion.

The 1-[(1*R*,2*S*,5*R*)-(−)-menthoxymethyl]-3-alkylimidazolium chlorides demonstrated an extremely high activity against microbes, with a wide spectrum of activity. The studied CILs also possess antielectrostatic properties, however, their effectiveness was dependent upon their state of aggregation at room temperature, which is related to the type of anion and length of the alkyl substituent on the imidazole ring. Thus, CILs not only represent new potential media for asymmetric synthesis, but also disinfectants with antielectrostatic activity.

Experimental

General methods

^{1}H NMR spectra were recorded on a Mercury Gemini 300 spectrometer operating at 300 MHz, with tetramethylsilane as the internal standard. ^{13}C NMR spectra were obtained with the same instrument at 75 MHz. Elemental analyses were performed at the A. Mickiewicz University, Poznań. Melting points were determined using a model JA 9100 electrothermal digital melting-point apparatus. Optical rotations were measured with a Perkin-Elmer 243 B polarimeter.

Glass transitions were measured using a Perkin-Elmer differential scanning calorimeter. The instrument temperature scale was calibrated at the crystal–crystal transition of cyclopentane (−151.16 °C) and the melting point of indium (+156.6 °C). Samples were sealed in aluminum pans and scanned at a rate of 20 K min^{-1} in a helium atmosphere. A Mettler Toledo DA 110 M scale was used for the mass/density measurements. A micro Ostwald viscometer was used for viscosity measurements. Simultaneous TG/DTA experiments were performed using a MOM (Hungary) Derivatograph-PC.

Syntheses

Chloromethyl (1*R*,2*S*,5*R*)-(−)-menthyl ether was prepared by passing HCl through a mixture of formaldehyde and (1*R*,2*S*,5*R*)-(−)-menthol, following the published method.[14]

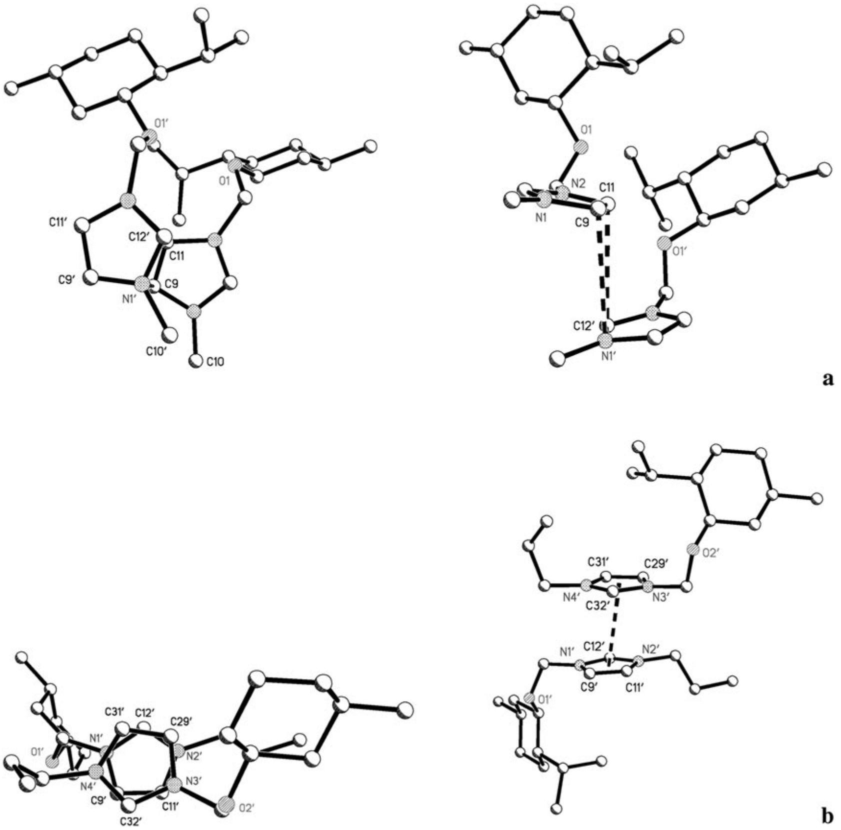

Fig. 6 π-Interactions in (a) **1a** · H_2O (top) and (b) **1c** · $0.5H_2O$ (bottom).

Preparation of 1-alkylimidazole. Imidazole (13.60 g, 0.20 mol) was carefully added to a solution of sodium (5 g, 0.22 mol) in 1-propanol (200 mL), and mixed by stirring in a round-bottomed flask, equipped with a magnetic stirring bar, a reflux condenser, and an addition funnel. Following the addition of imidazole, the mixture was heated at reflux to form a clear solution. The solution was cooled to room temperature and 150 mL of chloroform was added. The organic phase was washed with distilled water, dried over (Na_2SO_4), concentrated by rotoevaporation, and distilled to give the corresponding 1-alkylimidazole.

General procedure for quaternization. Chloromethyl (1*R*,2*S*,5*R*)-(−)-menthyl ether (0.02 mol) was added dropwise into a round-bottomed flask which contained a vigorously stirred mixture of 30 mL dry hexane and freshly distilled 0.02 mol of 1-alkylimidazole (in the case: 1,2-dimethylimidazole or 1-benzylimidazole, dry DMF or dry acetone was used, respectively). The reaction mixture was stirred at room temperature for 30 min. Then, the phases were separated and the crude product was washed twice with dry hexane (2 × 30 mL). The volatile materials were removed under reduced pressure at 60 °C overnight.

1-[(1*R*,2*S*,5*R*)-(−)-Menthoxymethyl]-3-ethylimidazolium chloride (1b). ^{1}H NMR (2D spectra) ($CDCl_3$, 25 °C): δ 0.49 (d, J = 7.1 Hz, 3H, H14 or H15), 0.88 (m, 9H, Ha-4, H7, H14 or H15, Ha-2 and Ha-1), 1.24 (m, 1H, H5), 1.43 (m, 1H, H3), 1.60 (m, 5H, Hb-1, Hb-4 and H16), 1.94 (sept d, J = 6.9 Hz, J = 4.7, 1H, H8), 2.12 (d, J = 12.0 Hz, 1H, Hb-2), 3.40 (td, J = 10.7 Hz, J = 4.4 Hz, 1H, H6), 4.47 (q, J = 14.8 Hz, J = 7.4 Hz, 2H, H10), 5.68 and 5.95 (d, J = 10.4 Hz, 2H, AB system, H13), 7.49 (t, J = 1.9 Hz, 1H, H11), 7.66 (t, J = 1.9 Hz, J = 1.6 Hz, 1H, H9), 11.06 (t, J = 1.1 Hz, 1H, H12); ^{13}C NMR ($CDCl_3$): δ 15.4 (C16), 15.5 (C14 or C15), 20.8 (C7), 22.0 (C14 or C15), 22.6 (C1), 25.3 (C8), 31.0 (C3), 33.9 (C4), 40.2 (C2), 45.3 (C10), 47.6 (C5), 76.6 (C6), 79.6 (C13), 121.0 (C11), 122.1 (C9), 137.6 (C12); elemental analysis: calc. (%) for $C_{16}H_{29}ClN_2O$ (300.87): C 63.87, H 9.72, N 9.31; found: C 64.02, H 9.63, N 9.01.

1-[(1*R*,2*S*,5*R*)-(−)-Menthoxymethyl]-3-methylimidazolium chloride (1a). ^{1}H NMR ($CDCl_3$, 25 °C): δ 0.52 (d, J = 6.9 Hz, 3H, H14 or H15), 0.89 (m, 9H, Ha-4, H7, H14 or H15, Ha-2 and Ha-1), 1.24 (m, 1H, H5), 1.42 (m, 1H, H3), 1.63 (m, 2H, Hb-1 and Hb-4), 1.95 (m, 1H, H8), 2.12 (m, 1H, Hb-2), 3.37 (td, J = 10.4 Hz, J = 4.4 Hz, 1H, H6), 4.16 (s, 3H, H10), 5.69, 5.89 (d, J = 10.4 Hz, 2H, AB system, H13), 7.54 (t, J = 1.9 Hz, J = 1.6 Hz, 1H, H11), 7.87 (t, J = 1.9 Hz, J = 1.6 Hz, 1H, H9), 10.72 (t, J = 1.2 Hz, 1H, H12); ^{13}C NMR ($CDCl_3$): δ 15.1 (C14 or C15), 20.4 (C7), 21.6 (C14 or C15), 22.3 (C1), 24.9 (C8), 30.6 (C3), 33.5 (C4), 36.2 (C10), 39.8 (C2), 47.2 (C5), 76.4 (C6), 79.1 (C13), 120.7 (C11), 124.0 (C9), 137.2 (C12); elemental analysis: calc. (%) for $C_{15}H_{27}ClN_2O$ (286.85): C 62.81, H 9.49, N 9.77; found: C 63.01, H 9.51, N 9.47.

1-[(1*R*,2*S*,5*R*)-(−)-Menthoxymethyl]-3-propylimidazolium chloride (1c). ^{1}H NMR ($CDCl_3$, 25 °C): δ 0.50 (d, J = 6.9 Hz, 3H, H14 or H15), 0.88 (m, 9H, Ha-4, H7, H14 or H15,

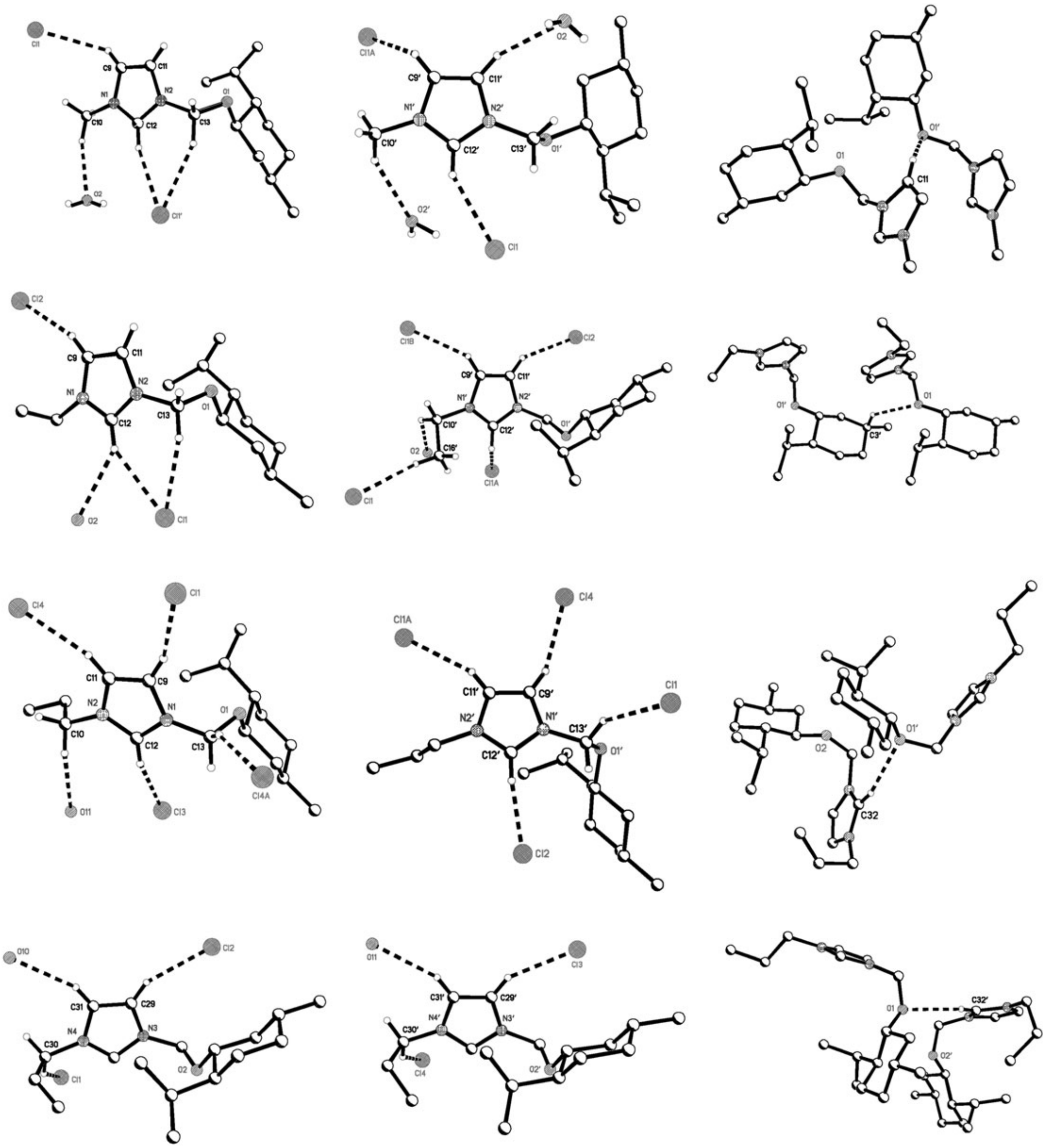

Fig. 7 Close contact environments for the cations in (a) **1a** · H_2O (top row); (b) **1b** · $0.5H_2O$ (second row); and (c) **1c** · $0.5H_2O$: O1, O1′ (third row), O2, O2′ (fourth row). Cation· · ·anion and cation· · ·water interactions are shown in columns one and two, cation· · ·cation interactions are shown in column three. Contacts shown are those at least −0.100 Å under the sum of the van der Waals radii.

Ha-2 and Ha-1), 1.23 (t, J = 3.6 Hz, 3H, H17), 1.28 (m, 1H, H5), 1.43 (m, 1H, H3), 1.58 (m, 2H, Hb-1 and Hb-4), 1.99 (m, 3H, H8 and H16), 2.11 (m, 1H, Hb-2), 3.41 (td, J = 10.4 Hz, J = 4.4 Hz, 1H, H6), 4.36 (t, J = 7.4 Hz, 2H, H10), 5.71 and 5.96 (d, J = 10.4 Hz, 2H, AB system, H13), 7.52 (t, J = 1.6 Hz, 1H, H11), 7.66 (t, J = 1.9 Hz, J = 1.6 Hz, 1H, H9), 11.01 (t, J = 1.2 Hz, 1H, H12); ^{13}C NMR ($CDCl_3$): δ 10.5 (C17), 15.5 (C14 or C15), 20.8 (C7), 21.9 (C14 or C15), 22.7 (C1), 23.5 (C16), 25.3 (C8), 31.0 (C3), 33.9 (C4), 40.3 (C2), 47.6 (C5), 51.5 (C10), 76.6 (C6), 79.8 (C13), 121.0 (C11), 122.4 (C9), 137.8 (C12); elemental analysis: calc. (%) for $C_{17}H_{31}ClN_2O$ (314.90): C 64.84, H 9.92, N 8.90; found: C 64.97, H 9.79, N 8.79.

1-[(1*R*,2*S*,5*R*)-(−)-Menthoxymethyl]-2,3-dimethylimidazolium chloride (1m). ^{1}H NMR ($CDCl_3$, 25 °C): δ 0.50 (d, J = 6.9 Hz, 3H, H14 or H15), 0.89 (m, 9H, Ha-4, H7, H14 or H15, Ha-2 and Ha-1), 1.22 (m, 1H, H5), 1.39 (m, 1H, H3), 1.63 (m, 2H, Hb-1 and Hb-4), 1.93 (m, 1H, H8), 2.08 (m, 1H, Hb-2), 2.83 (s, 3H, H27), 3.29 (td, J = 10.7 Hz, J = 4.4 Hz, 1H, H6), 4.03 (s, 3H, H10), 5.68 and 5.73 (d, J = 10.9 Hz, 2H, AB system, H13), 7.79 (d, J = 1.9 Hz 1H, H11), 7.90 (d, J = 1.9 Hz, 1H, H9); ^{13}C NMR ($CDCl_3$): δ 10.3 (C27), 15.3 (C14 or C15), 20.6 (C7), 21.9 (C14 or C15), 22.5 (C1), 25.2 (C8), 31.0 (C3), 33.8 (C4), 35.5 (C10), 40.0 (C2), 47.5 (C5), 76.0 (C6), 79.0 (C13), 121.5 (C11), 122.7 (C9), 144.8 (C12); elemental analysis: calc. (%) for $C_{16}H_{29}ClN_2O$ (300.87): C 63.87, H 9.72, N 9.31; found: C 63.72, H 9.93, N 9.29.

1-[(1*R*,2*S*,5*R*)-(−)-Menthoxymethyl]-3-benzylimidazolium chloride (1n). ^{1}H NMR ($CDCl_3$, 25 °C): δ 0.39 (d, J = 6.9 Hz, 3H, H14 or H15), 0.86 (m, 9H, Ha-4, H7, H14 or H15, Ha-2

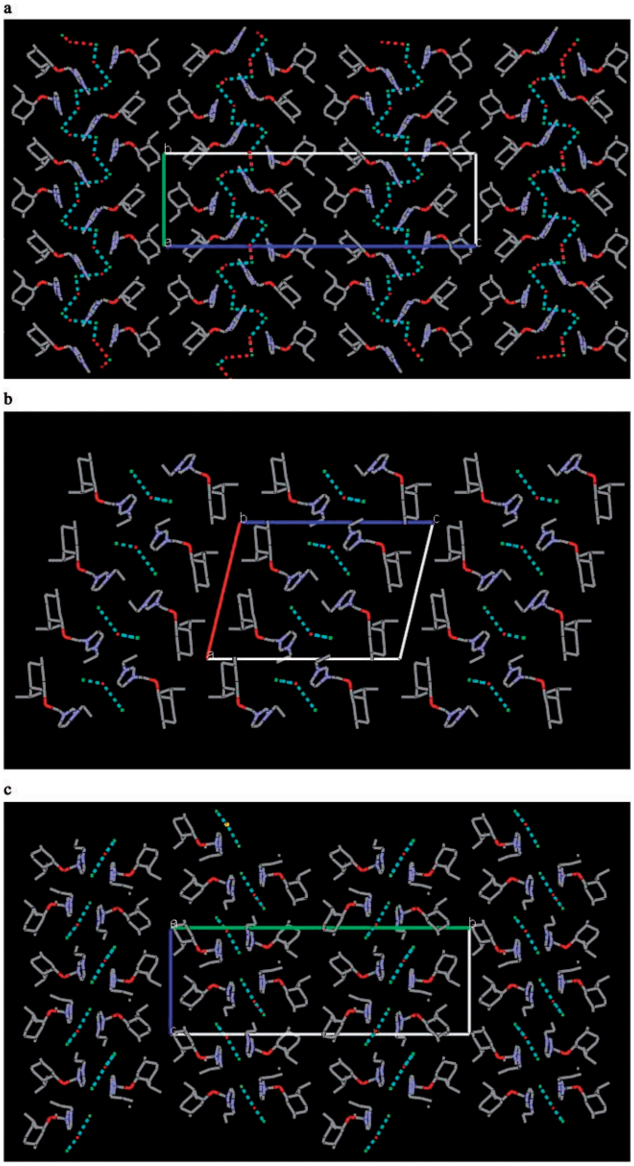

Fig. 8 Packing diagrams for (a) **1a** · H_2O (top, viewed down *a*), (b) **1b** · $0.5H_2O$ (middle, viewed down *a*), and (c) **1c** · $0.5H_2O$ (bottom, viewed down *c*), illustrating the orientation of the cations into hydrophobic menthol regions and hydrophilic imidazolium regions, and the strong chloride···water hydrogen bonds in light blue (a polymeric chain in **1a** · H_2O and discrete units in **1b** · $0.5H_2O$ and **1c** · $0.5H_2O$).

and Ha-1), 1.21 (m, 1H, H5), 1.44 (m, 1H, H3), 1.60 (m, 2H, Hb-1 and Hb-4), 1.88 (m, 1H, H8), 2.04 (m, 1H, Hb-2), 3.38 (td, *J* = 10.4 Hz, *J* = 4.1 Hz, 1H, H6), 5.63 (s, 3H, H10), 5.67 and 5.88 (d, *J* = 10.4 Hz, *J* = 10.7 Hz, 2H, AB system, H13), 7.37 (m, 3H, H11 and Ph), 7.50 (m, 4H, H9 and Ph), 11.11 (m, 1H, H12); ^{13}C NMR ($CDCl_3$): *δ* 15.3 (C14 or C15), 20.7 (C7), 21.9 (C14 or C15), 22.6 (C1), 25.2 (C8), 30.9 (C3), 33.8 (C4), 40.2 (C2), 47.5 (C5), 58.3 (C10), 76.6 (C6), 79.9 (C13), 121.6 (C11), 122.9 (C9), 128.9 (Ph), 129.3 (Ph), 129.4 (Ph), 133.9 (Ph), 137.7 (C12); elemental analysis: calc. (%) for $C_{21}H_{31}ClN_2O$ (362.99): C 69.48, H 8.62, N 7.72; found: C 69.63, H 8.59, N 7.61.

General procedure for ion exchange. Chiral imidazolium chlorides were dissolved in water or methanol and a saturated aqueous solution of inorganic salt was added. The reaction mixture was stirred at room temperature producing a heterogeneous mixture. The crude product was separated and washed with distilled water until chloride ions were no longer detected using $AgNO_3$. The obtained salt was dried at 80 °C for 24 h in vacuum.

In the cases of water-soluble salts, the water was first evaporated and the remnants were dissolved in dry acetone. The inorganic salt was separated and the solvent was evaporated to obtain the product.

1-[(1*R*,2*S*,5*R*)-(−)-Menthoxymethyl]-3-methylimidazolium tetrafluoroborate (2a). ^1H NMR ($CDCl_3$, 25 °C): *δ* 0.50 (d, *J* = 6.7 Hz, 3H, H14 or H15), 0.97 (m, 9H, Ha-4, H7, H14 or H15, Ha-2 and Ha-1), 1.29 (m, 1H, H5), 1.43 (m, 1H, H3), 1.61 (m, 2H, Hb-1 and Hb-4), 1.97 (m, 2H, H8 and Hb-2), 3.30 (td, *J* = 10.7 Hz, *J* = 4.4 Hz, 1H, H6), 3.97 (s, 3H, H10), 5.52, 5.60 (d, *J* = 10.4 Hz, 10.7 Hz, 2H, AB system, H13), 7.44 (t, *J* = 1.9 Hz, *J* = 1.6 Hz, 1H, H11), 7.46 (t, *J* = 1.9 Hz, *J* = 1.6 Hz, 1H, H9), 8.90 (t, *J* = 1.1 Hz, 1H, H12); ^{13}C NMR ($CDCl_3$): *δ* 15.3 (C14 or C15), 20.9 (C7), 22.0 (C14 or C15), 22.6 (C1), 25.2 (C8), 31.0 (C3), 33.9 (C4), 36.3 (C10), 39.9 (C2), 47.7 (C5), 76.6 (C6), 79.5 (C13), 121.3 (C11), 124.0 (C9), 136.3 (C12); elemental analysis: calc. (%) for $C_{15}H_{27}BF_4N_2O$ (338.20): C 53.27, H 8.05, N 8.27; found: C 53.39, H 8.29, N 8.40.

1-[(1*R*,2*S*,5*R*)-(−)-Menthoxymethyl]-3-methylimidazolium perchlorate (3). ^1H NMR ($CDCl_3$, 25 °C): *δ* 0.51 (d, *J* = 7.14 Hz, 3H, H14 or H15), 0.98 (m, 9H, Ha-4, H7, H14 or H15, Ha-2 and Ha-1), 1.25 (m, 1H, H5), 1.49 (m, 1H, H3), 1.63 (m, 2H, Hb-1 and Hb-4), 1.95 (m, 1H, H8), 2.03 (m, 1H, Hb-2), 3.32 (td, *J* = 10.4 Hz, *J* = 6.3 Hz, *J* = 4.1 Hz, 1H, H6), 4.01 (s, 3H, H10), 5.53, 5.63 (d, *J* = 10.4 Hz, *J* = 10.7 Hz 2H, AB system, H13), 7.46 (m, 2H, H11 and H9), 9.03 (t, *J* = 1.0 Hz, 1H, H12); ^{13}C NMR ($CDCl_3$): *δ* 15.4 (C14 or C15), 20.9 (C7), 22.1 (C14 or C15), 22.6 (C1), 25.3 (C8), 31.0 (C3), 33.9 (C4), 36.6 (C10), 40.0 (C2), 47.7 (C5), 76.6 (C6), 79.6 (C13), 121.4 (C11), 124.0 (C9), 136.5 (C12); elemental analysis: calc. (%) for $C_{15}H_{27}ClN_2O_5$ (350.84): C 51.35, H 7.76, N 7.98; found: C 51.29, H 7.66, N 7.79.

1-[(1*R*,2*S*,5*R*)-(−)-Menthoxymethyl]-3-methylimidazolium iodide (4). ^1H NMR ($CDCl_3$, 25 °C): *δ* 0.53 (d, *J* = 6.9 Hz, 3H, H14 or H15), 0.90 (m, 9H, Ha-4, H7, H14 or H15, Ha-2 and Ha-1), 1.26 (m, 1H, H5), 1.47 (m, 1H, H3), 1.63 (m, 2H, Hb-1 and Hb-4), 2.03 (m, 1H, H8), 2.16 (m, 1H, Hb-2), 3.41 (td, *J* = 10.7 Hz, *J* = 4.4 Hz, 1H, H6), 4.17 (s, 3H, H10), 5.69, 5.89 (d, *J* = 10.4 Hz, 2H, AB system, H13), 7.56 (t, *J* = 1.9 Hz, 1H, H11), 7.71 (t, *J* = 1.9 Hz, *J* = 1.7 Hz, 1H, H9), 10.39 (t, *J* = 1.0 Hz, 1H, H12); ^{13}C NMR ($CDCl_3$): *δ* 15.6 (C14 or C15), 20.8 (C7), 22.0 (C14 or C15), 22.7 (C1), 25.3 (C8), 31.0 (C3), 33.9 (C4), 37.1 (C10), 40.2 (C2), 47.6 (C5), 76.6 (C6), 79.7 (C13), 121.3 (C11), 124.0 (C9), 137.0 (C12); elemental analysis: calc. (%) for $C_{15}H_{27}IN_2O$ (378.30): C 47.63, H 7.19, N 7.41; found: C 47.54, H 7.28, N 7.33.

1-[(1*R*,2*S*,5*R*)-(−)-Menthoxymethyl]-3-methylimidazolium hexafluorophosphate (5). ^1H NMR ($CDCl_3$, 25 °C): *δ* 0.50 (d, *J* = 6.9 Hz, 3H, H14 or H15), 0.88 (m, 9H, Ha-4, H7, H14 or H15, Ha-2 and Ha-1), 1.24 (m, 1H, H5), 1.43 (m, 1H, H3),

Table 6 MIC and MBC values (μM) of 1-[(1*R*,2*S*,5*R*)-(−)-menthoxymethyl]-3-alkylimidazolium chlorides

		Chloride												
Strain		**1a**	**1b**	**1c**	**1d**	**1e**	**1f**	**1g**	**1h**	**1i**	**1j**	**1k**	**1l**	BAC[a]
M. luteus	MIC	28	53	25	12	5.8	2.8	1.3	0.5	0.25	< 0.25	< 0.25	< 0.25	1.4
	MBC	216	> 1664	51	189	91	174	84	21	5	2.4	2.3	1.1	11
S. aureua	MIC	873	832	397	94	47	11	22	2.6	1.3	0.5	4.7	0.2	2.8
	MBC	> 1745	> 1664	795	381	365	174	84	21	5	2.4	4.7	1.1	23
S. epidermidis	MIC	216	832	51	49	23	5.6	5.4	2.6	1.3	2.4	2.3	2.3	1.4
	MBC	> 1745	> 1664	795	381	730	45	22	5.2	1.3	2.4	2.3	4.5	5.6
E. faecium	MIC	> 1745	1664	795	189	91	45	22	5.2	2.5	0.5	1.2	1.1	5.6
	MBC	> 1745	> 1664	> 1590	1522	730	351	84	42	10	19	9.4	1.1	23
M. catarrhalis	MIC	436	416	197	94	47	11	5.4	2.6	1.3	2.4	0.5	< 0.25	0.6
	MBC	873	416	397	94	91	45	43	5.2	1.3	2.4	2.3	< 0.25	1.4
E. coli	MIC	436	103	99	49	23	2.8	1.3	1.3	0.5	2.4	2.3	0.5	2.8
	MBC	436	103	99	49	23	11	2.7	1.3	0.5	2.4	2.3	1.1	2.8
S. marcescens	MIC	> 1745	> 1664	> 1590	> 1522	1460	701	337	161	78	75	145	70	175
	MBC	> 1745	> 1664	> 1590	> 1522	1460	701	675	161	78	75	145	141	175
P. vulgaris	MIC	> 1745	> 1664	> 1590	> 1522	1460	701	337	81	40	9.7	9.4	9.1	88
	MBC	> 1745	> 1664	> 1590	> 1522	1460	701	337	161	40	19	9.4	18	88
P. aeruginosa	MIC	> 1745	> 1664	> 1590	> 1522	> 1460	701	337	161	40	39	73	70	175
	MBC	> 1745	> 1664	> 1590	> 1522	> 1460	1403	675	161	78	75	73	70	175
B. subtilis	MIC	873	1664	397	94	91	22	22	5.2	1.3	1.2	2.3	< 0.25	2.8
	MBC	873	1664	795	189	91	22	22	5.2	1.3	1.2	2.3	< 0.25	2.8
C. albicans	MIC	> 1745	> 1664	> 1590	> 1522	730	174	84	21	2.5	9.7	19	2.3	11
	MBC	> 1745	> 1664	> 1590	> 1522	1460	351	167	21	2.5	9.7	19	9.1	88
R. rubra	MIC	> 1745	> 1664	1590	> 1522	730	87	84	42	5	19	19	2.3	23
	MBC	> 1745	> 1664	1590	> 1522	> 1460	701	675	42	20	19	19	4.5	88

[a] Benzalkonium chloride.

1.62 (m, 2H, Hb-1 and Hb-4), 1.97 (m, 2H, H8 and Hb-2), 3.29 (td, *J* = 10.7 Hz, *J* = 4.4 Hz, 1H, H6), 3.94 (s, 3H, H10), 5.49, 5.55 (d, *J* = 10.4 Hz, *J* = 10.7 Hz, 2H, AB system, H13), 7.36 (t, *J* = 1.9 Hz, *J* = 1.6 Hz, 1H, H11), 7.41 (t, *J* = 1.9 Hz, *J* = 1.6 Hz, 1H, H9), 8.65 (t, *J* = 1.1 Hz, 1H, H12); ^{13}C NMR ($CDCl_3$): δ 15.3 (C14 or C15), 20.9 (C7), 22.0 (C14 or C15), 22.7 (C1), 25.3 (C8), 30.9 (C3), 34.0 (C4), 36.3 (C10), 39.9 (C2), 47.8 (C5), 76.6 (C6), 79.7 (C13), 121.3 (C11), 123.9 (C9), 136.0 (C12); elemental analysis: calc. (%) for $C_{15}H_{27}F_6N_2OP$ (396.36): C 45.46, H 6.87, N 7.07; found: C 45.56, H 6.91, N 7.21.

1-[(1*R*,2*S*,5*R*)-(−)-Menthoxymethyl]-3-methylimidazolium acesulfamate (6). ^{1}H NMR ($CDCl_3$, 25 °C): δ 0.48 (d, *J* = 7.1 Hz, 3H, H14 or H15), 0.87 (m, 9H, Ha-4, H7, H14 or H15, Ha-2 and Ha-1), 1.21 (m, 1H, H5), 1.39 (m, 1H, H3), 1.61 (m, 2H, Hb-1 and Hb-4), 1.99 (m, 5H, H8, Hb-2 and anion H28), 3.31 (td, *J* = 10.4 Hz, *J* = 4.4 Hz, 1H, H6), 4.05 (s, 3H, H10), 4.45 (s, 1H, anion H29), 5.60 and 5.74 (d, *J* = 10.4 Hz, 2H, AB system, H13), 7.52 (t, *J* = 1.9 Hz, *J* = 1.6 Hz, 1H, H11), 7.57 (t, *J* = 1.9 Hz, *J* = 1.6 Hz, 1H, H9), 9.87 (t, *J* = 1.0 Hz, 1H, H12); ^{13}C NMR ($CDCl_3$): δ 15.2 (C14 or C15), 20.7 (C7), 21.8 (C14 or C15), 22.5 (C1), 25.0 (C8), 30.8 (C3), 33.7 (C4), 36.1 (C10), 39.8 (C2), 47.4 (C5), 76.4 (C6), 79.0 (C13), 121.0 (C11), 123.6 (C9), 137.0 (C12); anion: 19.6 (C28), 101.8 (C29), 160.4 (C30), 169.3 (C31); elemental analysis: calc. (%) for $C_{19}H_{31}N_3O_5S$ (413.63): C 55.17, H 7.57, N 10.16; found: C 55.07, H 7.64, N 10.40.

1-[(1*R*,2*S*,5*R*)-(−)-Menthoxymethyl]-3-methylimidazolium trifluoroacetate (7). ^{1}H NMR ($CDCl_3$, 25 °C): δ 0.48 (d, *J* = 6.9 Hz, 3H, H14 or H15), 0.87 (m, 9H, Ha-4, H7, H14 or H15, Ha-2 and Ha-1), 1.23 (m, 1H, H5), 1.39 (m, 1H, H3), 1.63 (m, 2H, Hb-1 and Hb-4), 1.94 (m, 1H, H8), 2.02 (m, 1H, Hb-2), 3.30 (td, *J* = 10.7 Hz, *J* = 4.4 Hz, 1H, H6), 4.04 (s, 3H, H10), 5.59 and 5.75 (d, *J* = 10.4 Hz, *J* = 10.7 Hz, 2H, AB system, H13), 7.58 (t, *J* = 1.9 Hz, *J* = 1.6 Hz, 1H, H11), 7.71 (t, *J* = 1.9 Hz, *J* = 1.6 Hz, 1H, H9), 10.26 (t, *J* = 1.0 Hz, 1H, H12);

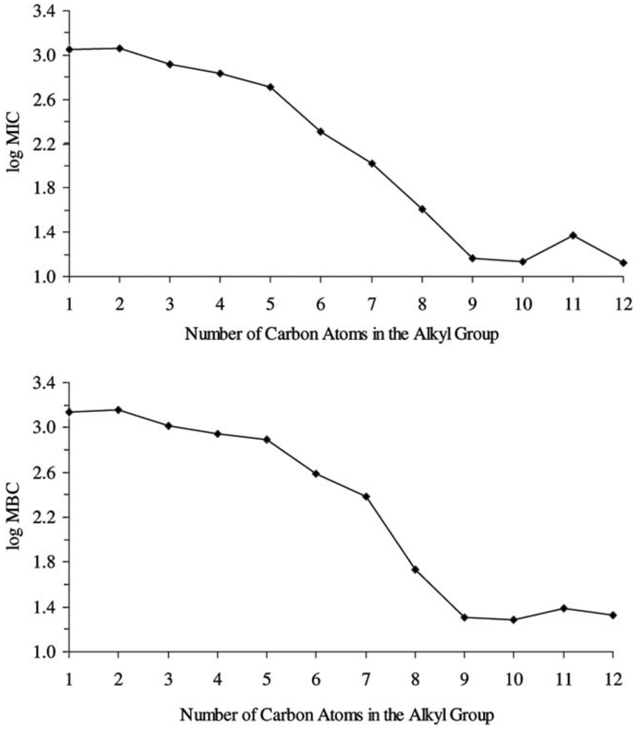

Fig. 9 Mean MIC values (top) and MBC values (bottom) for microorganisms.

Table 7 Criteria for the estimation of the antielectrostatic effect based on the surface resistance R_s (Ω) and half-charge decay time $\tau_{1/2}$ (s)

log R_s	$\tau_{1/2}$/s	Antielectrostatic effect
<9	<0.5	Excellent
9–9.9	0.51–2	Very good
10–10.9	2.1–10	Good
11–11.9	10.1–100	Sufficient
12–12.9	>100	Insufficient
>13	>600	No antielectrostatic properties

^{13}C NMR (CDCl$_3$): δ 14.8 (C14 or C15), 20.4 (C7), 21.5 (C14 or C15), 22.2 (C1), 24.8 (C8), 30.6 (C3), 33.5 (C4), 35.7 (C10), 39.5 (C2), 47.2 (C5), 76.2 (C6), 78.9 (C13), 121.0 (C11), 123.8 (C9), 137.5 (C12); anion: 114.9, 118.8 (C28), 159.8, 160.3, 160.7, 161.1 (C29); elemental analysis: calc. (%) for $C_{17}H_{27}F_3N_2O_3$ (364.46): C 56.02, H 7.48, N 7.69; found: C 56.17, H 7.52, N 7.55.

1-[(1*R*,2*S*,5*R*)-(−)-Menthoxymethyl]-3-methylimidazolium bis(trifluoromethanesulfonyl)imide (8a). ^{1}H NMR (CDCl$_3$, 25 °C): δ 0.50 (d, J = 6.9 Hz, 3H, H14 or H15), 0.88 (m, 9H, Ha-4, H7, H14 or H15, Ha-2 and Ha-1), 1.25 (m, 1H, H5), 1.40 (m, 1H, H3), 1.63 (m, 2H, Hb-1 and Hb-4), 2.04 (m, 2H, H8 and Hb-2), 3.28 (td, J = 10.7 Hz, J = 4.4 Hz, 1H, H6), 3.97 (s, 3H, H10), 5.52, 5.59 (d, J = 10.4 Hz, 2H, AB system, H13), 7.46 (t, J = 1.9 Hz, J = 1.6 Hz, 1H, H11), 7.48 (t, J = 1.9 Hz, J = 1.6 Hz, 1H, H9), 8.87 (t, J = 1.0 Hz, 1H, H12); ^{13}C NMR (CDCl$_3$): δ 15.0 (C14 or C15), 20.6 (C7), 21.7 (C14 or C15), 22.6 (C1), 25.2 (C8), 30.9 (C3), 33.8 (C4), 36.1 (C10), 39.8 (C2), 47.5 (C5), 76.6 (C6), 79.7 (C13), 121.6 (C11), 124.1 (C9), 135.7 (C12); anion: 113.3, 117.5, 121.8, 126.0; elemental analysis: calc. (%) for $C_{17}H_{27}F_6N_3O_5S_2$ (531.67): C 38.40, H 5.13, N 7.91; found: C 38.45, H 5.30, N 7.76.

Test microorganisms. The microorganisms were: *Micrococcus luteus* NCTC 7743, *Staphylococcus aureus* NCTC 4163, *Staphylococcus epidermidis* ATCC 49134, *Enterococcus faecium* ATCC 49474, *Moraxella catarrhalis* ATCC 25238, *Escherichia coli* ATCC 25922, *Serratia marcescens* ATCC 8100, *Proteus vulgaris* NCTC 4635, *Pseudomonas aeruginosa* NCTC 6749, *Bacillus subtilis* ATCC 6633, *Candida albicans* ATCC 10231, *Rhodothorula rubra* (Demml 1889, Lodder 1934). Standard strains were supplied by the National Collection of Type Cultures (NCTC) and London and American Type Culture Collection (ATCC). *Rhodothorula rubra* was obtained from the Department of Pharmaceutical Bacteriology, University of Medical Sciences, Poznań.

Antimicrobial activity test procedure. Antimicrobial activity was determined by the tube dilution method. A series of chiral imidazolium chloride dilutions was prepared in Müller–Hinton broth medium (bacteria) or Sabouraud broth medium (fungi). Bacteria strains were cultured in Müller-Hinton broth for 24 h and fungi in Sabouraud agar for 48 h. A suspension of the microorganisms, at a concentration of 10^6 cfu mL^{-1}, were prepared from each culture and each dilution of the broth medium was inoculated with one of the above-mentioned suspensions in a 1 : 1 ratio. Growth (or lack thereof) of the microorganisms was determined visually after incubation for 24 h at 37 °C (bacteria) or 48 h at 28–30 °C (fungi). The lowest concentration, at which there was no visible growth (turbidity), was taken as the MIC. Then, from each tube, one loopful was cultured on an agar medium with inactivates (0.3% lecithin, 3% polysorbate 80, and 0.1% cysteine L) and incubated for 48 h at 37 °C (bacteria) or for 5 d at 28–30 °C (fungi). The lowest concentration of chiral imidazolium salt supporting no colony formation was defined as the MBC.

Antielectrostatic properties

The antielectrostatic effect was measured on a Wigofil polyethylene film with a density of 150 g m^{-2} that did not contain any lubricants or antioxidants. From this 0.25 mm film, 12.5 mm diameter disks were cut. The disks were washed in acetone and then dried by placing them in an air-conditioned room.

Table 8 Surface resistance R_s (Ω), half-charge decay time $\tau_{1/2}$ (s), and antielectrostatic effect for the chiral imidazolium salts

Salt	log R_s	$\tau_{1/2}$	Effect	Salt	log R_s	$\tau_{1/2}$	Effect
1a	8.3	0.25	Excellent	**2h**	>13	>600	None
1b	8.0	0.25	Excellent	**2i**	>13	>600	None
1c	7.7	0.25	Excellent	**2j**	>13	>600	None
1d	8.3	0.45	Excellent	**2k**	>13	>600	None
1e	8.0	0.25	Excellent	**2l**	>13	>600	None
1f	8.6	0.45	Excellent	**3**	>13	>600	None
1g	7.3	<0.1	Excellent	**4**	10	0.35	Good
1h	7.7	0.2	Excellent	**5**	>13	>600	None
1i	7.8	0.2	Excellent	**7**	7.8	0.2	Excellent
1j	7.5	<0.1	Excellent	**8a**	9.9	0.9	Very good
1k	7.5	0.2	Excellent	**8b**	9.5	0.95	Very good
1l	7.6	0.2	Excellent	**8c**	9.5	0.75	Very good
1m	12	>100	Insufficient	**8d**	9.6	0.35	Very good
1n	10.0	8.7	Good	**8e**	9.3	0.55	Very good
2a	>13	>600	None	**8f**	9.5	0.75	Very good
2b	>13	>600	None	**8g**	9	0.3	Very good
2c	12.3	>100	Insufficient	**8h**	9	0.25	Very good
2d	12.0	>100	Insufficient	**8i**	8.8	0.2	Excellent
2e	>13	>600	None	**8j**	9.8	0.9	Very good
2f	>13	>600	None	**8k**	9.5	0.55	Very good
2g	>13	>600	None	**8l**	9.8	0.95	Very good

A disk was rubbed on the surface with a cotton-swab soaked with a 0.5% chloroform solution of each studied salt. Then, the disk was hung up so that the chloroform could evaporate spontaneously.

The disks, covered with chiral imidazolium salts, were stored for 24 h in an air-conditioned room at 20 ± 2 °C and a relative humidity of 55 ± 5%. Finally, the surface resistance and half-life decay time were measured. The measuring apparatus and the method have recently been described elsewhere.[32] The relative error in the determination of these two quantities did not exceed 5%.

X-Ray crystallography

Data were collected on a Bruker CCD area detector-equipped diffractometer with graphite monochromated Mo-Kα (λ = 0.71073 Å) radiation and the structures solved using the SHELXTL software package.[33] Absorption corrections were made with SADABS.[34] The structures were refined by full-matrix least-squares on F^2. Details unique to each structure are discussed below.

Data collection and structure refinement for crystals of **1a**·H_2O proceeded normally. The initial unit cell determination resulted in the orthorhombic space group $P2_12_12_1$, and the atoms were readily located from the initial structure solution. The positions of all non-hydrogen atoms were anisotropically refined and the hydrogen atoms were located from the Fourier difference map and refined isotropically.

Suitable crystals of **1b**·$0.5H_2O$ were selected by determination of unit cell parameters for several crystals and analyzing the standard deviations and the goodness-of-fit parameters. The initial structure solution in the monoclinic space group $P2_1$ resulted in large thermal parameters for the ethyl group on the imidazole ring (C10, C16, C10′ and C16′) and for the solvent water oxygen (O10), indicating possible disorder or high thermal motion. An adequate disorder model could not be resolved and the refinement proceeded with full weighted atoms. Hydrogen atoms (except for those on O10) were placed in calculated positions 0.95 Å from the bonded carbon atom and allowed to ride on that atom with U fixed at $1.2 \times U_{eq}$ of the carbon atom. The hydrogen atoms on the solvent water molecule could not be located and thus, were not included in the final refinement. Additional crystals of **1b**·$0.5H_2O$ were screened and the best data set was used in the final refinement.

Suitable crystals of **1c**·$0.5H_2O$ were also selected by determination of unit cell parameters and analyzing the standard deviations and the goodness-of-fit parameters for several crystals. The initial unit cell determination resulted in the orthorhombic space group $P2_12_12$, however, closer examination indicated the possibility of a monoclinic space group, $P2_1$. The non-hydrogen atoms were readily located, but high thermal parameters were noted for the terminal carbon atoms on the *n*-propyl groups attached to the imidazole rings (C37A/B and C37C/D) and for C34′ and C35′ in the isopropyl group on one of the menthol groups. The disorder on the *n*-propyl groups was resolved with two positions for each disordered carbon atoms, each at 50% occupancy. These disordered atoms were refined in alternate least-squares cycles. An adequate disorder model could not be resolved for the isopropyl C34′ and C35′ atoms and the refinement proceeded with full weighted atoms. Hydrogen atoms (except for those on O10 and O11) were placed in calculated positions 0.95 Å from the bonded carbon atom and allowed to ride on that atom with U fixed at $1.2 \times U_{eq}$ of the bonded atom. The hydrogen atoms on the solvent water molecules could not be located and are not included in the final refinement. Additional crystals of **1c**·$0.5H_2O$ were screened with careful review of the unit cell and merging R value for the equivalent data; the best data set was used in the final refinement.

Crystal data for 1a·H_2O. $C_{15}H_{29}ClN_2O_2$, M = 304.85, orthorhombic, space group $P2_12_12_1$, a = 8.2722(11), b = 11.2447(16), c = 37.776(5) Å, V = 3513.8(8) Å^3, T = 173 K, Z = 8, μ(Mo-Kα) = 0.221 mm^{-1}, 22 770 reflections measured, 8353 unique, R_1 = 0.0486, wR_2 = 0.0765 [$I > 2\sigma(I)$].

Crystal data for 1b·$0.5H_2O$. $C_{16}H_{30}ClN_2O_{1.5}$, M = 309.87, monoclinic, space group $P2_1$, a = 13.0143(14), b = 8.0671(8), c = 17.9287(18) Å, β = 103.636(2)°, V = 1829.2(3) Å^3, T = 173 K, Z = 4, μ(Mo-Kα) = 0.212 mm^{-1}, 11 927 reflections measured, 7007 unique, R_1 = 0.0565, wR_2 = 0.1478 [$I > 2\sigma(I)$].

Crystal data for 1c·$0.5H_2O$. $C_{17}H_{32}ClN_2O_{1.5}$, M = 323.90, monoclinic, space group $P2_1$, a = 9.4408(10), b = 34.119(4), c = 12.1754(13) Å, β = 90.292(2)°, V = 3921.8(7) Å^3, T = 173 K, Z = 8, μ(Mo-Kα) = 0.200 mm^{-1}, 25 348 reflections measured, 17 434 unique, R_1 = 0.0672, wR_2 = 0.1432 [$I > 2\sigma(I)$].

CCDC reference numbers 613884–613886 (**1a–1c**).

For crystallographic data in CIF or other electronic format see DOI: 10.1039/b616215k

Acknowledgements

This work was supported by the COST D29 working group D29/0015/04 and at The University of Alabama by the U.S. Environmental Protection Agency's STAR program through grant number RD-83143201. (Although the research described in this article has been funded in part by EPA, it has not been subjected to the Agency's required peer and policy review and therefore does not necessarily reflect the views of the Agency and no official endorsement should be inferred.)

References

1 *Ionic Liquids III A/B: Fundamentals, Progress, Challenges, and Opportunities*, ed. R. D. Rogers and K. R. Seddon, *ACS Symp. Ser.*, American Chemical Society, Washington, DC, 2005, vol. 901/902.
2 J. Howarth, K. Hanlon, D. Fayne and P. McCormac, *Tetrahedron Lett.*, 1997, **38**, 3097–3100.
3 M. J. Earle, P. B. McCormac and K. R. Seddon, *Green Chem.*, 1999, **1**, 23–25.
4 P. Wasserscheid, A. Bösmann and C. Bolm, *Chem. Commun.*, 2002, 200–201.
5 Y. Ishida, H. Miyauchi and K. Sago, *Chem. Commun.*, 2002, 2240–2241.
6 Y. Haramoto, T. Miyashita, M. Nanasawa, Y. Aoli and H. Nohira, *Liq. Cryst.*, 2002, **29**, 87–90.

7 W. Bao, Z. Wang and Y. Li, *J. Org. Chem.*, 2003, **68**, 591–593.
8 J. Levilain, G. Dubant, I. Abrunhosa, M. Gulea and A.-C. Gaumont, *Chem. Commun.*, 2003, 2914–2915.
9 C. Baudequin, J. Baudoux, J. Levillain, D. Cahard, A.-C. Gaumont and J.-C. Plaquevent, *Tetrahedron: Asymmetry*, 2003, **14**, 3081–3093.
10 G. V. Thanh, B. Pegot and A. Loupy, *Eur. J. Org. Chem.*, 2004, 1112–1116.
11 J. Pernak, I. Goc and I. Mirska, *Green Chem.*, 2004, **6**, 323–329.
12 J. J. Jodry and K. Mikami, *Tetrahedron Lett.*, 2004, **45**, 4429–4431.
13 N. Jain, A. Kumar, S. Chauhan and S. M. S. Chauhan, *Tetrahedron*, 2005, **61**, 1015–1060.
14 J. Pernak and J. Feder-Kubis, *Chem. Eur. J.*, 2005, **11**, 4441–4449.
15 J. Baudoux, P. Judeinstein, D. Cahard and J.-C. Plaquevent, *Tetrahedron Lett.*, 2005, **46**, 1137–1140.
16 B. Ni, A. D. Headley and G. Li, *J. Org. Chem.*, 2005, **70**, 10600–10602.
17 E. J. Kim, S. Y. Ko and E. K. Dziadulewicz, *Tetrahedron Lett.*, 2005, **46**, 631–633.
18 F. Guillen, D. Brégeon and J.-C. Plaquevent, *Tetrahedron Lett.*, 2006, **47**, 1245–1248.
19 H. Xue, R. Verma and J. M. Shreeve, *J. Fluorine Chem.*, 2006, **127**, 159–176.
20 J. Ding and D. W. Armstrong, *Chirality*, 2005, **17**, 281–292.
21 B. Pegot, G. Vo-Thanh, D. Gori and A. Loupy, *Tetrahedron Lett.*, 2004, **45**, 6425–6428.
22 R. Gausepohl, P. Buskens, J. Kleinen, A. Bruckmann, C. W. Lehmann, J. Klankermayer and W. Leitner, *Angew. Chem., Int. Ed.*, 2006, **45**, 3689–3692.
23 J. Ding, V. Desikan, X. Han, T. L. Xiao, R. Ding, W. S. Jenks and D. W. Armstrong, *Org. Lett.*, 2005, **7**, 335–337.
24 K. Fukumoto, M. Yoshizawa and H. Ohno, *J. Am. Chem. Soc.*, 2005, **127**, 2398–2399.
25 G. Tao, L. He, N. Sun and Y. Kou, *Chem. Commun.*, 2005, 3562–3564.
26 J. Pernak and J. Feder-Kubis, *Tetrahedron: Asymmetry*, 2006, **17**, 1728–1737.
27 K. R. Seddon, A. Stark and M.-J. Torres, *Pure Appl. Chem.*, 2000, **72**, 1391–1398.
28 J. Pernak, K. Sobaszkiewicz and J. Foksowicz-Flaczyk, *Chem. Eur. J.*, 2004, **10**, 3479–3485.
29 T. Liebert and T. Heinze, *Biomacromolecules*, 2005, **6**, 333–340.
30 A. A. Fannin, Jr, L. A. King, J. A. Levisky and J. S. Wilkes, *J. Phys. Chem.*, 1984, **88**, 2609–2614.
31 J. Pernak, K. Sobaszkiewicz and I. Mirska, *Green Chem.*, 2003, **5**, 52–56.
32 J. Pernak, A. Czepukowicz and R. Poźniak, *Ind. Eng. Chem. Res.*, 2001, **40**, 2379.
33 G. M. Sheldrick, *SHELXTL*, Version 5.05, Siemens Analytical X-Ray Instruments, Inc., Madison, WI, 1996.
34 G. M. Sheldrick, *Program for Semiempirical Absorption Correlation of Area Detector Data*, University of Göttingen, Germany, 1996.